Journal Pre-proofs

Hardware Article

PAW, a cost-effective and open-source alternative to commercial rodent running wheels

Dylan J. Terstege, Jonathan R. Epp

Please cite this article as: D.J. Terstege, J.R. Epp, PAW, a cost-effective and open-source alternative to commercial rodent running wheels, *HardwareX* (2023), doi: https://doi.org/10.1016/j.ohx.2023.e00499

Article title

PAW, a cost-effective and open-source alternative to commercial rodent running wheels

Authors

Dylan J. Terstege[1*] & Jonathan R. Epp[1]

Affiliations

[1]Department of Cell Biology and Anatomy, Hotchkiss Brain Institute, Cumming School of Medicine, University of Calgary, 3330 Hospital Drive NW, Calgary, Alberta, Canada T2N 4N1.

Corresponding author's email address and Twitter handle

Dylan.Terstege@ucalgary.ca

Twitter: @dterstege

Abstract

Voluntary wheel running is a common measure of general activity in many rodent models across neuroscience and physiology. However, current commercial wheel monitoring systems can be cost-prohibitive to many investigators, with many of these systems requiring investments of thousands of dollars. In recent years, several open-source alternatives have been developed, and while these tools are much more cost effective than commercial system, they often lack the flexibility to be applied to a wide variety of projects. Here, we have developed PAW, a 3D Printable Arduino-based Wheel logger. PAW is wireless, fully self-contained, easy to assemble, and all components necessary for its production can be obtained for only $75 CAD. Furthermore, with its compact internal electronics, the 3D printed casing can be easily modified to be used with a wide variety of running wheel designs for a wide variety of rodent species. Data recorded with the PAW system shows circadian patterns of activity which is expected from mice and is consistent with results found in the literature. Altogether, PAW is a flexible, low-cost system that can be beneficial to a broad range of researchers who study rodent models.

Specifications table

Hardware name	PAW; Printable Arduino-base Wheel logger
Subject area	• Neuroscience
Hardware type	• Measuring physical properties and in-lab sensors
Closest commercial analog	*Med Associates Low-Profile Wireless Running Wheel* *https://med-associates.com/product/low-profile-wireless-running-wheel/*
Open-source license	GNU General Public License v3.0
Component Acquisition Expense	$75 CAD
Source file repository	Zenodo: https://doi.org/10.5281/zenodo.8408545 A live version of the repository can be found on GitHub: https://github.com/dterstege/PAW/

1. Hardware in context

When running wheels are made available in the wild, wheel running has been observed as being a natural rodent behavior [1]. In the laboratory, home cage voluntary wheel-running has a rich history in neuroscience research involving rodents. As a metric, voluntary wheel running has been commonly used to assess motricity in rodents, which has provided novel insights on strain-specific differences in activity and has proven to be a valuable marker of improved health in several disease models [2–6]. Additionally, voluntary wheel running has been shown to be useful in the study of circadian rhythms [7]. As an intervention, access to voluntary wheel running is commonly used as a means of introducing enrichment and opportunity for exercise[8–13]. In both cases, the ability to record and track wheel revolutions over time is important.

Currently, there are several commercial systems which allow for the tracking of voluntary running activity over time in the home cage; however, these systems are often cost-prohibitive and/or require users to purchase expensive propriety software licenses. The closest commercial analog to these wheels, the Low-Profile Running Wheel from Med Associates (#ENV-047), requires the additional purchase of a wireless communication hub (Wireless Device USB Hub, #DIG-807), data acquisition software (Wheel Manager Data Acquisition Software, #SOF-860), and a computer to manage these components. Consequently, this configuration can easily cost thousands of dollars.

While open-source alternatives exist, the majority of these have been designed with specific experimental parameters in mind, which may not suit the needs of most researchers. For example, many of the open-source low-profile running wheels which have previously been published are not wireless, and therefore require a wired connection to pass through the cage from the wheel to an external computer/power source. This may not be a major concern in certain cage configurations[14]; however, this may be prohibitive to other researchers who do not have access to these cages. Furthermore, in other designs in which wires are passed through the cage, the wire is vulnerable to damage from chewing which can incur data loss. Alternatively, other open-source low-profile running wheels may use sensors outside of the cage to monitor activity[15]. While this design is accessible and not prone to damage from chewing, it requires the wheel to remain in a specific location within the home cage relative to the external sensor and does not have much tolerance. As the speed of wheel revolution increases, it is not uncommon for wheels to move slightly around the cage. This movement could easily shift the wheel outside of the read range of an sensors fixed to the outside of a cage. Therefore, while this running wheel design may be suitable for some experiments, it presents the potential for data loss. Oftentimes, even the open-source low-profile running wheels which address these issues through integrated on-board sensors and a wireless design require additional postprocessing through additional software packages to produce meaningful data[16]. In table 1, PAW is compared to several other low-profile, open-source mouse running wheels across several practical measures.

Table 1. Low-Profile Open-Source Mouse Running Wheel Comparison

Running Wheel	Component Acquisition Expense - $CAD	Power Source	Data Storage	Cage Modifications	Resolution	Data Output

PAW	$75	Battery-powered	On-board MicroSD	None	0.01s	CSV
Open Face Home Cage Running Wheel [17]	$89	External Power Source	On-board MicroSD	Requires hole through which a USB power cable can be passed	Not specified	CSV
DynaLok [14]	$144 (Laptop not included)	External Power Source	External Laptop	Requires hole through which a USB power cable can be passed	1s	CSV
Motricity Tracker [15]	$99 (Laptop not included)	External Power Source	External Laptop	None; but does require wheel to be fixed in position next to an external sensor	0.25s	TXT
LOST-Wheel [18]	$40 (Laptop not included)	External Power Source	External Laptop	Requires hole through which a USB power cable can be passed	1s	Custom Analysis Needed
WRAQ [19]	$75	Battery-powered	On-board MicroSD	None	4s	Custom Analysis Needed
MRC [20]	$50	Battery-powered	On-board Counter; No Data Export	None	Not specified	None; Manual Logging from Display

With these issues in mind, the most broadly useful open-source low-profile running wheel should be simple and inexpensive to build, should have a wireless design which is able to fit within the dimension of most used mouse cages, should have on-board sensors, and the output data files should require minimal, if any, postprocessing to yield meaningful data. In this manuscript, we describe the PAW, a Printable Arduino-based Wheel logger designed to meet these criteria.

2. Hardware description

PAW is an inexpensive, freely accessible, and open-source alternative to commercially available wireless low-profile running wheels. This running wheel facilitates the monitoring of voluntary wheel running in the home cage, reducing the stress caused by moving mice to other arenas for voluntary exercise. Its design fits comfortably in most standard mouse cages (PAW dimensions: height: 8.57 cm; width: 15.24 cm; depth: 15.24 cm). The low-profile nature of the wheel promotes a more natural spine angle than traditional, upright, vertical running wheels, and minimizes risk of injury making this system considerably safer as a long-term source of voluntary exercise [21].

PAW is easy to assemble and requires only very basic soldering and 3D printing abilities. None of the manufacturing process requires particularly advanced tools, with an entry-level 3D printer being more than sufficient to build the external casing. Alternatively, if users do not wish to purchase their own 3D printer or do not have access to such equipment, many companies offer 3D printing services and will have no problems printing PAW components (e.g., Prototype Hubs, Craftcloud, Shapeways, etc.). All components of the PAW are contained within this 3D-printed case which fits securely under the base of the commercially available Mouse Igloo, rendering the system completely wireless and not reliant upon proximity to external sensors. The output files of the PAW are stored to an on-board MicroSD present data as an easy-to-read CSV file for immediate use without the need for further processing. Furthermore, the compact design of the electrical components within the PAW design allows for considerable build flexibility. With modifications to the 3D-printed case, the PAW could be very easily adapted for use with a variety of wheel designs, including the larger low-profile saucer-style wheels compatible with rats and hamsters. Altogether, these features make the PAW a unique and accessible new tool for neuroscientists and physiologists alike.

The PAW is suitable for tracking running wheel revolutions in most mouse home cage configurations, making it particularly useful for researchers interested in:

- Exercise Physiology
- Motoric Recovery
- Home Cage Enrichment

Design files

3. Print settings

All STL files listed in Table 1 were printed using a Creality Ender 3 V2 3D printer, with all slicing having been conducted in Ultimaker Cura (v4.8.0). Print specifications include 1.75 mm PLA material extruded through a 0.4 mm brass nozzle at a layer height of 0.12 mm, 50% infill, 1.2 mm perimeter wall thickness and support structures with a minimum overhang angle of 59 degrees. These layer heights were chosen to increase the resolution of the logo on the front of the PAW system. Increasing this layer height to 0.28 mm may compromise the aesthetic of this logo, but is one means through which the duration of the printing process can be reduced considerably without compromising the overall integrity of the printed components.

The Ender 3 V2 3D printer was equipped with a frosted glass build plate, which was cleaned with acetone followed by 100% isopropyl alcohol prior to each print. The brass nozzle of the 3D printer was cleaned with acetone prior to each print. The printing speed for each component was set to 40 mm/s, to ensure proper layer adhesion with the current manufacturing setup. The speed at which these components can be printed will vary from printer to printer. The provided estimates of speed and total printing time are conservative, and it is likely that many other manufacturing setups will be able to reliably accommodate printing these components at higher speeds.

4. Design files summary

Table 2. Design files summary

Design file name	File type	Open-source license	Location of the file
Dome, v1	F3D (Fusion 360), STL	GPL3.0	https://doi.org/10.5281/zenodo.8408545
Base, v1	F3D (Fusion 360), STL	GPL3.0	https://doi.org/10.5281/zenodo.8408545

PAW, v2	Arduino IDE	GPL3.0	https://doi.org/10.5281/zenodo.8408545

Dome

The Dome is the top portion of the 3D-printed case housing the electronics within the PAW. The dimensions of this component have been designed to fit securely within the base of the Bio-Serv Mouse Igloo. This component requires approximately 69 g (23.29 m) of 1.75 mm PLA to print.

Base

The Base is the bottom portion of the 3D-printed case housing the electronics within the PAW. This component is secured to the Dome with three M3x8 screws. This component requires approximately 29 g (9.85 m) of 1.75 mm PLA to print.

Code

This Arduino IDE file contains the code responsible for programming the PAW. This file has been commented in full to help users understand the purpose of each line in the code. These comments also indicate which lines of the code are to be modified by the user, such as the date and the time to be read by the real time clock.

Bill of materials

5. **Bill of materials summary**

Designator	Component	Quantity	Cost per unit - $CAD	Total cost - $CAD	Source of materials	Material type
Mouse Igloo	Bio-Serv Mouse Igloo (K3570)	1	$4.05	$4.05	Bio-Serv	

Fast-Trac Wheel	Bio-Serv Fast-Trac (K3251)	1	$6.15	$6.15	Bio-Serv	
Arduino Microcontroller	Arduino Uno R3	1	$20.95	$20.95	3D Printing Canada	
Hall Sensor	Hall Effect Magnetic Sensor (KY-003)	1	$5.56	$5.56	Amazon	
Real-Time Clock (RTC)	Real Time Clock Module (DS321)	1	$5.40	$5.40	Amazon	
MicroSD Reader	MicroSD Card Reader Module	1	$2.46	$2.46	Amazon	
Boost Converter	T64 DC to DC Step Up Voltage Module	1	$1.31	$1.31	Amazon	
Battery Holder	3 AA Battery Holder	1	$2.96	$2.96	Amazon	
AA Batteries	High-Capacity Rechargeable AA Batteries	3	$3.00	$9.75	Amazon	
CR2032 Battery	Lithium CR2032 Battery	1	$1.71	$1.71	Amazon	

MicroSD Card	32 GB High Speed MicroSD Card	1	$4.40	$4.40	Amazon	
Silicone Wire	22 AWG Silicone Wire	105 cm	$0.05 /10 cm	$5.25	Amazon	Copper
Magnet	Magnet	1	$0.43	$0.43	Amazon	Ferrite
3D Printing Filament	1.75 mm PLA Filament	98 g	$0.03 /g	$2.94	Amazon	PLA
M3x8 Screw	M3x8 Screw	3	$0.11	$0.33	Amazon	Stainless Steel
M3x12 Screw	M3x8 Screw	4	$0.12	$0.48	Amazon	Stainless Steel

Solder and flux were applied as needed while assembling the electronics. Heat shrink tubing was applied to junctions between Silicone Wires. Electrical tape was used to cover on-board LEDs on the Arduino Microcontroller and the RTC. Non-toxic hot glue was used to adhere the Magnet to the underside of the Fast-Trac wheel.

6. Build instructions

This section has the following subsections:

6.1. 3D Printing

6.2. Electronics Assembly

6.3. Full Assembly

6.4. Ease of Manufacturing

6.1. 3D Printing

    I.   Download the appropriate STL files from the PAW GitHub page.

II. Generate g-code compatible with your 3D printer. In our case, we used a Creality Ender 3 v2 3D printer and g-code was generated using Ultimaker Cura (4.8.0)

III. Print both components (Dome and Base). Combined, these components can be printed in two days or less, depending on the manufacturing setup being used during this process.

6.2. Electronics Assembly

I. *De-solder pin headers*. The Hall Effect Sensor, RTC, and MicroSD Reader modules often come with male pin headers already soldered into the boards (as shown in Fig. 1A. In Fig. 1I these pins have been removed). These male pin headers add unnecessary bulk to the build and will prevent components from fitting within the 3D-printed case. Ensure that the MicroSD card is not in the MicroSD Reader and that the CR2032 Battery is not in the RTC during these procedures.

   a. Note: some Hall Effect Sensor modules have an on-board LED. To minimize light disturbance in the home cage, it is advised that users remove this LED and re-solder a connection between its attachment points on the Hall Effect Sensor module.

II. *Pre-cut lengths of Silicone Wire*. As a guide, fifteen 7 cm lengths of wire can be prepared in advance. Each end of these lengths can be stripped to expose approximately 7 – 8 mm of wire, enough to securely attach to the headers of the Arduino Microcontroller. We recommend having at least 6 different colors of wire available to easily distinguish between connections. It is also recommended that consistent colors are used throughout (e.g., red wire for power; black wire for ground).

III. *Prepare wires for junctions*. There are three junction points at which multiple wires need to be soldered together: two of which are between two pairs of ground wires and one of which is between a pair of power wires. Each of these junctions is described below:

   a. Cut one of the ground wires down to approximately 3 cm and strip 1 cm of silicone coating away from this end. From a second ground wire, strip the silicone coating from 2 – 2.5 cm to expose a junction point for these two wires (Fig. 1B). Wrap the longer of the exposed ends of the smaller ground wire segment around this exposed junction (Fig. 1C). This will result in a junction with 3 ends and will allow for two components to connect to a single ground port on the Arduino Microcontroller. Solder this junction together and cover the connection with shrink wrap tubing once complete (Fig. 1D).

   b. Repeat the procedures outlined above with two more segments of ground wire to make another separate junction with 3 ends (Fig. 1B,C). This will allow for two more components to connect to a separate ground port on the Arduino Microcontroller. Cover this connection with shrink wrap tubing once complete (Fig. 1D).

   c. From two power wires, strip the silicone coating from 3 – 3.5 cm to expose a junction point (Fig. 1E). Wrap these wires around each other at these exposed points to create a junction with 4 ends (Fig. 1F). This will allow for

3 components to be powered by a single output voltage port on the Arduino Microcontroller. Solder this junction together and cover this connection with shrink wrap tubing once complete (Fig. 1G).

IV. *Insert power and ground wires into their appropriate headers on the Arduino Microcontroller*. For each of the ground wire junctions, the shortest end is inserted into a ground (GND) port. Insert one of these ground wire junctions on each side of the Arduino Microcontroller. One of the two equally short ends of the power wire junction is inserted into the 5V port.

V. *Arrange and prepare components around the board*. See Fig. 1H for a schematic depicting the organization of these components and Fig. 1I for a photograph of this wiring. All LEDs on the Arduino Microcontroller and the RTC should be covered with electrical tape at this time.

VI. *Trim wires for appropriate component placement*. In many cases, the pre-cut length of 6 cm is excessive; however, it allows for flexibility when organizing the placement of components. Wires can now be inserted into the ports of the Hall Effect Sensor, RTC, MicroSD Reader, and Boost Converter. It is recommended that users begin with power and ground wires, as other connections have fewer dependencies and can thus be arranged more flexibly.
   a. Note: to ensure a secure connection between the Battery Holder and the Arduino Microcontroller, it may be necessary to solder the ground wire of the Battery Holder to a short length of Silicone Wire, which will have a larger AWG and will hold more securely in the header of the Arduino Microcontroller.

VII. *Soldering wires to appropriate components*. With wires trimmed to appropriate lengths to minimize the footprint of the electronics, users can begin soldering connections, applying flux as needed. As with the de-soldering steps, ensure that the MicroSD card is not in the MicroSD Reader and that the CR2032 Battery is not in the RTC during these procedures. Additionally, ensure that the AA batteries are not in the Battery Holder.

6.3. Full Assembly

Once the electronics have been assembled and the 3D printed components have been generated, the PAW can be assembled in full (Fig. 2). First, flash the Arduino IDE script from the Code section of the GitHub repository to the Arduino Microcontroller. Instructions for the use of this code are outlined in full in the *Operation instructions* section of this manuscript. With the Arduino Microcontroller now running the appropriate code, batteries and microSD cards can now be inserted into the electronics in the following order (which will ensure that the Arduino Microcontroller does not attempt to write to a non-existent MicroSD card):

I. One CR2032 Battery is inserted into the RTC.
II. One MicroSD Card is inserted into the MicroSD reader.
III. Three AA Batteries are inserted into the Battery Holder.

With the electronics now fully operational, four M3x12 Screws are inserted through the holes in the center of the underside of the Base (Fig. 2B). Turning this component over, these screws align with the holes on the Arduino Microcontroller board. Carefully press the Arduino Microcontroller onto the base, passing these screws through the holes of the board (Fig. 2C). These screws will secure the Arduino Microcontroller in place within the 3D-printed case. Next, the Battery Holder can be arranged on top of the Arduino Microcontroller. This allows for the Dome to be placed over-top of the entire assembly. The Base is secured to the Dome with 3 M3x8 Screws on the underside of the Base (Fig. 2D). The final step of this build is to assemble the Bio-Serv Mouse Igloo with Fast-Trac and then use non-toxic hot glue to secure a magnet to the underside of the Fast-Trac wheel (Fig. 2E-G).

In some experimental designs, control groups will be given running wheels identical to those being used for the running manipulation; however, these wheels will be locked to prevent wheel revolutions. This serves as a control for the presence of a novel object within the home cage. The Bio-Serv Mouse Igloo equipped with the Fast-Trac wheel do not include an inherent locking mechanism and as such is not incorporated into our design. However, this same effect can be obtained by applying hot glue to the connection points on the pin which connects these two components. This will effectively but non-permanently prevent the wheel from rotating.

6.4. Ease of Manufacturing

The assembly time of each running wheel is limited by the duration of the 3D printing. When operating the 3D printer at conservative printing speeds, the construction of each wheel requires approximately 48 hours. All assembly of the electronic components can be completed in under one hour, independent of the 3D printing. None of the individual steps in these procedures require particular technical prowess and have all been completed with relative ease by individuals with minimal experience with the assembly of electronics.

7. Operation instructions

This section has the following subsections:

7.1. Programming the Arduino Microcontroller

7.2. Accessing and Analyzing Data

7.3. Other Considerations

7.1. Programming the Arduino Microcontroller

Download and install the Arduino IDE (https://www.arduino.cc/en/software). Once installed, open the application, and navigate to "Manage Libraries…" in the Tools menu and install the following libraries:

    I.   RTClib
   II.   SD

RTClib contains the module DS3231, which will allow for us to use the RTC, while SD contains modules which will allow for reading and writing to the MicroSD card.

With these libraries installed, users can now connect the Arduino to their computer using a USB B cable. After this, the Code file can now be opened. When a user clicks on a line of the code in the Arduino IDE, the line number will appear in the bottom left corner of the application, this function can be helpful in finding lines of interest within a script. Lines 55 and 56 contain variables for setting the time and date of the RTC. Users should modify line 55 to the present time as hh, mm, ss (hour, minutes, seconds) in 24-hour format. In line 56, time date should be set as dd, mm, yyyy (day, month, year). For example, the lines below show the RTC being set to 5:30 PM on October 31st, 2023:

```
rtc.setTime(17, 30, 00);

rtc.setDate(31, 10, 2023);
```

After the date and time have been accurately modified in the script, the code can now be uploaded to the Arduino Microcontroller. In the Tools tab of the Arduino IDE, set "Boards" to "Arduino Uno" and "Port" to "COM (Arduino Uno)". Finally, compile and upload the code to the Arduino Microcontroller by pressing the sideways arrow icon in the IDE.

7.2. Accessing and Analyzing Data

To access and analyze wheel revolution data, users simply need to unscrew the Base of the PAW and remove the MicroSD card. The MicroSD card will contain a CSV file for each day that the PAW system has been logging data. Each of these files which contains the timestamp at which each wheel revolution occurred with 1/100 s resolution.

While these data do not inherently require further processing, the CSV formatting renders further analyses (e.g., revolutions per hour) very easily indexable by commonly used programming IDEs.

7.3. Other Considerations

Battery Life: While the use of a wireless running wheel such as PAW reduces clutter from additional cables and cage modifications, they are not without their limitations. The primary concern when using a wireless running wheel is the battery life. As these wheels continuously read the signal from the hall effect sensor, they are constantly drawing power. From our testing, using 3000 mAh AA lithium batteries (EBL), data was able to be recorded for 4 consecutive days without need to replace batteries. When using 2800 mAh rechargeable AA batteries (EBL), data was able to be recorded for 2 consecutive days without loss. This is roughly the same amount of time as the same batteries are able to power the commercially available *Med Associates Low-Profile Wireless Running Wheel*. However, battery lifetime will vary depending on the batteries being used. Therefore, it is recommended that users of the PAW system assess battery health frequently (every 1 – 2 days) during and replace batteries accordingly to minimize the potential for missed recordings.

Sanitization and Durability: The durability of the 3D printed casing is largely influenced by the temperament of mice using the PAW system and the parameters applied during the printing process. Using the printing parameters outlined in the current manuscript, PAW systems easily withstood 4 weeks of continuous use with only minor signs of wear. With a durable and reusable device, it is also important to consider the actions that can be taken to sanitize the PAW system. In the current system, the PAW casing was printed using polylactic acid (PLA), a thermoplastic with a low glass transition temperature in the range of 60 °C. Potential sanitization options may vary with different 3D printing materials and settings. Largely, PLA-printed components are resilient to chemical cleaning with Cidex OPA, ethylene oxide, ethanol, hydrogen peroxide, peracetic acid, and chlorine solutions [22–25]. 3D-printed components have also been demonstrated to be able to withstand sterilization through gamma and ultraviolet radiation with only minor structural changes [24,26]. Low-temperature vapour sterilization has been shown to induce changes in the impact strength of PLA-printed components; however, no gross malformations are expected [23]. Additionally, many vapour sterilization techniques are also compatible with electronics and can therefore be conducted while the electronic components of the PAW system are within the 3D-printed case. Autoclave and dry heat sterilization techniques are not recommended, as the temperatures required for these methods will often result in considerable deformation to PLA-printed components [23]. For the current experiments, the 3D-printed components of

the PAW system were cleaned with 70% ethanol solution and sterilized using ultraviolet radiation.

Space in the Home Cage: Running wheels provide considerable enrichment in the home cages of laboratory rodents; however, they also occupy considerable space. Building from the commercially available Bio-Serv Mouse Igloo and Fast-Trac Wheel, the PAW system fits comfortably in two commonly used home cage designs (Fig. 2H,I). At housing densities of 5 mice per cage, there were no obvious differences in the behavior of mice house with the PAW system and those who had not. Mice were also provided with nesting materials and a paper housing dome (SS-Dome; Shepherd Specialty Papers). However, housing density and the presence of other forms of enrichment in the home cage is often regulated by institutional regulatory agencies. Undertaking any experimental protocol requires adherence to institutional guidelines for laboratory safety. These guidelines may differ from one institution to the next. Readers will need to acquire permissions from their relevant institutions prior to conducting these experiments.

8. Validation and characterization

To test the performance of the PAW, we assessed whether these wheels would reveal a pair of well-established observations in mouse wheel running. Firstly, it is expected that, without prior acclimation, wheel running should increase as mice familiarize themselves with the running wheels. Secondly, it is expected that running should fluctuate over the course of 24 hours in accordance with mouse circadian rhythm, with most wheel revolutions occurring during when lights are off in the housing facility.

Running wheels were provided for one week to cages of 8-week-old male and female C57BL/6J mice (n = 6 cages of male mice, 5 mice per cage; and 6 cages of female mice, 5 mice per cage). Wheels were provided in the home cage under otherwise standard laboratory housing conditions with *ad libitum* access to food and water. Mice were kept on a 12:12 light:dark cycle (lights on at 08:00). All experiments were conducted in accordance with the Canadian Council on Animal Care guidelines and with the approval of the University of Calgary Animal Care Committee.

Mice were not acclimated to running wheels beforehand; however, wheel revolutions were recorded even on their first day with the PAW. Wheel running was assessed in terms of distance travelled per hour. For comparisons of running by hour of the day, the

mean number of wheel revolutions was assessed for each cage across the duration of the 7-day experiment at each hour. For comparisons of wheel running activity during the light and dark phases of the light cycle, the mean number of revolutions during each of these phases was assessed for each cage across the duration of the 7-day experiment.

Using the PAW, we were able to observe rhythmic changes in running activity over the course of the day (Fig. 3A). Consistent with previous reports [27,28], wheel running increased during the dark phase and decreased during the light phase (Fig. 3B, Two-Factor ANOVA; phase effect, $F_{(1,20)}$ = 108.8, $p < 0.0001$). Also consistent with previous reports [21,29], running increased over time as mice became more familiar with the running wheels (Fig. 3C, Two-Factor ANOVA; day effect, $F_{(6,70)}$ = 5.317, $p = 0.0001$). Furthermore, daily running distance was within the expected range of 4 – 20 km per mouse, per day [21,30].

These results highlight the ability of the PAW system to dependably monitor and record wheel running activity in laboratory mice.

Ethics statements

All experiments complied with the ARRIVE guidelines and were conducted in accordance with the Canadian Council on Animal Care guidelines and with the approval of the University of Calgary Animal Care Committee.

CRediT author statement

Dylan J. Terstege: Conceptualization, Methodology, Software, Hardware, Visualization, Writing – Original draft preparation, Writing – Reviewing and editing. **Jonathan R. Epp:** Conceptualization, Writing – Original draft preparation, Writing – Reviewing and editing, Supervision.

Declaration of Competing Interest

The authors declare that they have no known competing financial interests or personal relationships that could have appeared to influence the work reported in this paper.

Acknowledgments

References:

[1] J.H. Meijer, Y. Robbers, Wheel running in the wild, Proc. Biol. Sci. 281 (2014) 20140210.

[2] A. Eltokhi, B. Kurpiers, C. Pitzer, Comprehensive characterization of motor and coordination functions in three adolescent wild-type mouse strains, Sci. Rep. 11 (2021) 1–12.

[3] D. Liebetanz, P. Baier, W. Paulus, K. Meuer, M. Bahr, J. Weishaupt, A highly sensitive automated complex running wheel test to detect latent motor deficits in the mouse MPTP model of Parkinson's disease, Exp. Neurol. 205 (2007) 207–213.

[4] T.C. Delorme, S.B. Srikanta, A.S. Fisk, M.-È. Cloutier, M. Sato, C.A. Pothecary, C. Merz, R.G. Foster, S.A. Brown, S.N. Peirson, N. Cermakian, G.T. Banks, Chronic exposure to dim light at night or irregular lighting conditions impact circadian behavior, motor coordination, and neuronal morphology, Front. Neurosci. 16 (2022). https://doi.org/10.3389/fnins.2022.855154.

[5] A. Tappe-Theodor, T. King, M.M. Morgan, Pros and cons of clinically relevant methods to assess pain in rodents, Neurosci. Biobehav. Rev. 100 (2019) 335–343.

[6] R. Kandasamy, A.T. Lee, M.M. Morgan, Depression of home cage wheel running: a reliable and clinically relevant method to assess migraine pain in rats, J. Headache Pain. 18 (2017). https://doi.org/10.1186/s10194-017-0721-6.

[7] D.M. Edgar, T.S. Kilduff, C.E. Martin, W.C. Dement, Influence of running wheel activity on free-running sleep/wake and drinking circadian rhythms in mice, Physiol. Behav. 50 (1991) 373–378.

[8] J.R. Epp, L.C.P. Botly, S.A. Josselyn, P.W. Frankland, Voluntary Exercise Increases Neurogenesis and Mediates Forgetting of Complex Paired Associates Memories, Neuroscience. 475 (2021) 1–9.

[9] G.A. Scott, D.J. Terstege, A.J. Roebuck, K.A. Gorzo, A.P. Vu, J.G. Howland, J.R. Epp, Adult neurogenesis mediates forgetting of multiple types of memory in the rat, Mol. Brain. 14 (2021) 97.

[10] A.R. Gobinath, R.J. Richardson, C. Chow, J.L. Workman, S.E. Lieblich, A.M. Barr, L.A.M. Galea, Voluntary running influences the efficacy of fluoxetine in a model of postpartum depression, Neuropharmacology. 128 (2018) 106–118.

[11]   G. Bastioli, J.C. Arnold, M. Mancini, A.C. Mar, B. Gamallo-Lana, K. Saadipour, M.V. Chao, M.E. Rice, Voluntary exercise boosts striatal dopamine release: Evidence for the necessary and sufficient role of BDNF, J. Neurosci. 42 (2022) 4725–4736.

[12]   A.C. Venezia, L.M. Guth, R.M. Sapp, E.E. Spangenburg, S.M. Roth, Sex-dependent and independent effects of long-term voluntary wheel running on Bdnf mRNA and protein expression, Physiol. Behav. 156 (2016) 8–15.

[13]   W. Zhou, J.C. Barkow, C.R. Freed, Running wheel exercise reduces α-synuclein aggregation and improves motor and cognitive function in a transgenic mouse model of Parkinson's disease, PLoS One. 12 (2017) e0190160.

[14]   K.A. Mayr, L. Young, L.A. Molina, M.A. Tran, P.J. Whelan, An economical solution to record and control wheel-running for group-housed mice, J. Neurosci. Methods. 331 (2020) 108482.

[15]   G.E. Deitzler, N.P. Bira, J.R. Davidson, M.M. David, An open-source, low-cost voluntary running activity tracking tool for in vivo rodent studies, PLoS One. 17 (2022) e0273865.

[16]   M. Zhu, D.K. Kasaragod, K. Kikutani, K. Taguchi, H. Aizawa, A novel microcontroller-based system for the wheel-running activity in mice, ENeuro. 8 (2021) ENEURO.0260-21.2021.

[17]   N. Godfrey, K. Chen, T. Tayyab, G. Dimitropoulos, F.P. MacMaster, S.L. Borgland, Development of an open face home cage running wheel for testing activity-based anorexia and other applications, ENeuro. 9 (2022) ENEURO.0246-22.2022.

[18]   J.J. Bivona, M.E. Poynter, An open-source, lockable mouse wheel for the accessible implementation of time- and distance-limited elective exercise, PLoS One. 16 (2021) e0261618.

[19]   M. Zhu, D.K. Kasaragod, K. Kikutani, K. Taguchi, H. Aizawa, A novel microcontroller-based system for the wheel-running activity in mice, ENeuro. 8 (2021) ENEURO.0260-21.2021.

[20]   J. Edwards, B. Olson, D.L. Marks, Constructing and programming a cost-effective murine running wheel with digital revolution counter, Lab Anim. (NY). 50 (2021) 202–204.

[21]   G. Manzanares, G. Brito-da-Silva, P.G. Gandra, Voluntary wheel running: patterns and physiological effects in mice, Braz. J. Med. Biol. Res. 52 (2019). https://doi.org/10.1590/1414-431x20187830.

[22]   J.C. Fleischer, J.C. Diehl, L.S.G.L. Wauben, J. Dankelman, The effect of chemical cleaning on mechanical properties of three-dimensional printed polylactic acid, J. Med. Device. 14 (2020). https://doi.org/10.1115/1.4046120.

[23]   R. Told, Z. Ujfalusi, A. Pentek, M. Kerenyi, K. Banfai, A. Vizi, P. Szabo, S. Melegh, J. Bovari-Biri, J.E. Pongracz, P. Maroti, A state-of-the-art guide to the sterilization of thermoplastic polymers and resin materials used in the additive manufacturing of medical devices, Mater. Des. 223 (2022) 111119.

[24]   J. Wiseman, T. Rawther, M. Langbart, M. Kernohan, Q. Ngo, Sterilization of bedside 3D-printed devices for use in the operating room, Annals of 3D Printed Medicine. 5 (2022) 100045.

[25]   T.M. Rankin, N.A. Giovinco, D.J. Cucher, G. Watts, B. Hurwitz, D.G. Armstrong, Three-dimensional printing surgical instruments: are we there yet?, J. Surg. Res. 189 (2014) 193–197.

[26]   S. Pérez Davila, L. González Rodríguez, S. Chiussi, J. Serra, P. González, How to sterilize polylactic acid based medical devices?, Polymers (Basel). 13 (2021) 2115.

[27]   J. Goh, W. Ladiges, Voluntary wheel running in mice, Curr. Protoc. Mouse Biol. 5 (2015) 283–290.

[28]   R.S. Bains, S. Wells, R.R. Sillito, J.D. Armstrong, H.L. Cater, G. Banks, P.M. Nolan, Assessing mouse behaviour throughout the light/dark cycle using automated in-cage analysis tools, J. Neurosci. Methods. 300 (2018) 37–47.

[29]   L. Garrett, D.C. Lie, M. Hrabé de Angelis, W. Wurst, S.M. Hölter, Voluntary wheel running in mice increases the rate of neurogenesis without affecting anxiety-related behaviour in single tests, BMC Neurosci. 13 (2012). https://doi.org/10.1186/1471-2202-13-61.

[30]   J.P. De Bono, D. Adlam, D.J. Paterson, K.M. Channon, Novel quantitative phenotypes of exercise training in mouse models, Am. J. Physiol. Regul. Integr. Comp. Physiol. 290 (2006) R926–R934.

Figures:

Figure 1: Electronics assembly. A. Photograph showing the components required for assembling the PAW system. To assemble the required ground wire junctions, (**B**) wire segments are trimmed and stripped, (**C**) wrapped around one another, (**D**) and soldered then wrapped with heat-shrink tubing. To assemble the required power wire junctions, (**E**) wire segments are stripped, (**F**) wrapped around one another, (**G**) and soldered then wrapped with heat-shrink tubing. **H**. Schematic showing the wiring of the necessary PAW components. **I**. Photograph of the fully soldered PAW system. **J**. Photograph of the fully assembled electronic component.

Figure 2: Full assembly of PAW. A. The Dome and Base components of the PAW system, 3D-printed with PLA. Four M3x12 screws were inserted into the base (**B**) which are then used to hold the electronics in place using the holes on the Arduino Microcontroller board (**C**). **D**. The Base is then secured to the Dome with three M3x8 screws. **E**. The Bio-Serv Mouse Igloo fits securely over the Dome. **F**. A strong magnet is glued to the inside of the Bio-Serv Fast-Trac wheel, (**G**) which is then mounted onto the Mouse Igloo. Fully assembled PAW systems in commonly used mouse laboratory home cages from (**H**) Ancare (N10 Mouse) and (**I**) Techniplast (GM500).

Figure 3: Experimental validation of PAW. Wheel running activity was assessed using PAW. **A**. Mean hourly running distance recorded from across one week for cages of male (n = 6 cages; 5 mice per cage) and female (n = 6 cages, 5 mice per cage) mice. Lights were turned on at ZT0 and turned off at ZT12. **B**. Male and female mice recorded greater running activity during the dark phase, while lights were off, than during the light phase. **C**. The mean distance travelled per cage increased over the course of the week.
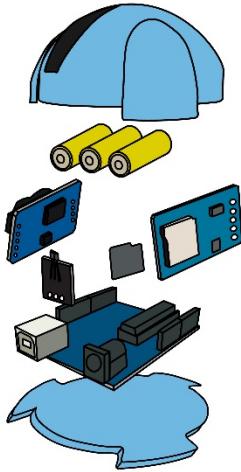
Dylan J. Terstege is a PhD candidate studying under the supervision of Dr. Jonathan Epp in the Cumming School of Medicine's Hotchkiss Brain Institute at the University of Calgary. His research focuses on understanding how intrinsic and extrinsic factors change neural circuits supporting memories.
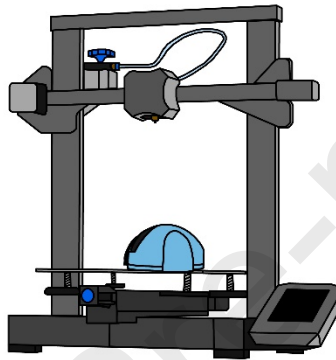
A

B

C